

Effect of purification treatment on properties of Mg-Gd-Y-Zr alloy

WANG Jie(王杰), ZHOU Ji-xue(周吉学), TONG Wen-hui(童文辉), YANG Yuan-sheng(杨院生)

Institute of Metal Research, Chinese Academy of Sciences, Shenyang 110016, China

Received 23 September 2009; accepted 30 January 2010

Abstract: Mg-Gd-Y-Zr alloy was purified by the method of filtering purification. The type, morphology, size distribution and volume fraction of inclusions in the alloy were analyzed using optical microscope and scanning electron microscope, and the effects of the inclusions on the mechanical and corrosion properties of the alloy were investigated. The results indicate that the filtering purification method is effective to remove inclusions in the alloy. By the filtering purification method, the average size of inclusions in the alloy reduces from 12.7 μm to 4.3 μm and the average volume fraction of inclusions in the alloy reduces from 0.26% to 0.06%. The ultimate tensile strength, yield strength and elongation of the alloy are improved from 200 MPa, 156 MPa and 3.4% to 232 MPa, 167 MPa and 7.0%, respectively. The corrosion rate of the alloy decreases dramatically from 38.8g/(m²·d) to 2.5 g/(m²·d) in the salt spray test.

Key words: Mg-Gd-Y-Zr alloy; purification treatment; inclusion; mechanical properties; corrosion resistance

1 Introduction

The magnesium alloys containing heavy rare earth elements have great application prospects in automotive, aircraft and aerospace industries for their high strength. In recent years, much effort has been devoted to develop Mg-Gd-Y-Zr alloys that are found to exhibit higher specific strength at both room and elevated temperatures and better creep resistance than other commercial Mg alloys[1]. However, due to their high chemical activities, magnesium and rare earth elements tend to oxidize rapidly during the process of smelting and casting, which results in burning loss of rare earth elements and formation of inclusions[2–3]. The inclusions destroy the continuity of the magnesium matrix, induce the defects such as pores and cracks, and impair the mechanical and corrosion properties of the alloy[4–5]. To reduce inclusions in magnesium alloys, several refining methods have been developed, including traditional flux refining and fluxless refining, such as inert gas, vacuum distillation refining and filtering refining[6–10]. Traditional flux refining is considered one of the most effective methods to remove the inclusions in magnesium alloys. However, MgCl₂ in the flux is easy to react with the rare earth elements Gd and Y in

magnesium alloys, which results in the loss of Gd and Y[11–12]. Meanwhile, the new flux inclusions are introduced into the alloy by using the flux, which results in bad corrosion behavior. Filtering is an efficient purification method and can remove not only large but also small inclusions in magnesium alloys effectively. It is propitious to magnesium alloys containing heavy rare earth elements because there is no loss of rare earth elements caused by flux. In addition, the filtration method is not detrimental to the environment and it will not introduce new inclusions into the alloy. Meanwhile, the refining process is supposed to be more economical than other processes.

In this study, a kind of Mg-Gd-Y-Zr alloy is purified by the method of filtering purification. In order to achieve high refining efficiency, stainless steel nets are introduced to filtering purification process. The effectiveness of the filtering purification is investigated and evaluated. Moreover, the mechanical and corrosion properties of the purified Mg-Gd-Y-Zr alloy are tested.

2 Experimental

2.1 Materials

The chemical composition (mass fraction, %) of the Mg-Gd-Y-Zr alloy used in the experiment was Gd 12.07,

Y 3.27, Zr 0.38, Fe <0.001, Cu 0.001, Ni <0.001, and balance Mg.

2.2 Smelting and refining

The alloy was melted in a 4 kW electric resistance furnace under the protection of a mixed gas consisting of SF₆ (0.5%, volume fraction) and CO₂ (99.5%, volume fraction). Before melting, the alloys and tools used in the experiments were heated to 200 °C in a baking oven in order to eliminate water. The melt was poured into a graphite mould through the preheated stainless steel nets at pouring temperature of 600 °C. The size of the ingot was d 48 mm×80 mm.

2.3 Mechanical properties test

Tensile specimens were taken from the ingots along the longitudinal direction. The ambient temperature tensile tests were carried out by a AG-100KNG materials testing machine at a crosshead speed of 1 mm/min. Three specimens under the same conditions were tested and the final values were obtained in terms of their average value.

2.4 Salt spray test

The salt spray tests, according to ASTM B117[13], were made to determine the corrosion performance of the samples. The size of specimens for salt spray tests was 25 mm×15 mm×4 mm. The specimens were polished on finer grades of emery papers up to 2 000 grit and then were cleaned with ethanol and acetone and dried. After that, the total surface area (S) and mass (m_0) of the specimens were measured. The specimens were put into the salt spray chamber at 35 °C. After six days, the specimens were taken out and cleaned in a solution of 15% Cr₂O₃+1% AgNO₃ in 500 mL of water in boiling condition for 5 min. Following that, the specimens were rinsed by acetone and distilled water and dried. The mass of the corroded specimen (m_c) was measured by an analytical balance. Then, the mass loss (m_L) and the corrosion rate (R) were calculated by the following equations:

$$m_L = m_0 - m_c \quad (1)$$

$$R = m_L / (S \cdot P) \quad (2)$$

where t is the immersion time.

2.5 Morphology observation and composition determination

The morphologies of inclusions in the ingots were observed with optical microscope (OM) on the cross-section. Statistical size and volume fraction of inclusions in metallographic specimens were measured by the SISC-IAS image software. Morphology of the corroded surface and fractographs of the tensile samples

were characterized using scanning electron microscope (SEM). The composition of inclusions was analyzed with energy dispersive spectroscope (EDS) attached to the SEM.

3 Results and discussion

3.1 Morphology and content of inclusions

The morphologies of inclusions in Mg-Gd-Y-Zr alloy with and without purification treatments are shown in Fig.1. The inclusions in the unpurified specimen are irregular and in cluster. After the purification treatments, the size of inclusions in the purified alloy decreases gradually compared with that in the unpurified alloy. The size and quantity of inclusions in the alloy decrease with the decrease of the filter pore size. When the filter pore size decreases from 425 μm to 150 μm, the cluster of inclusions disappears and finer inclusions exist in the alloy. The bigger inclusions are removed and the finer inclusions distribute evenly in the alloy.

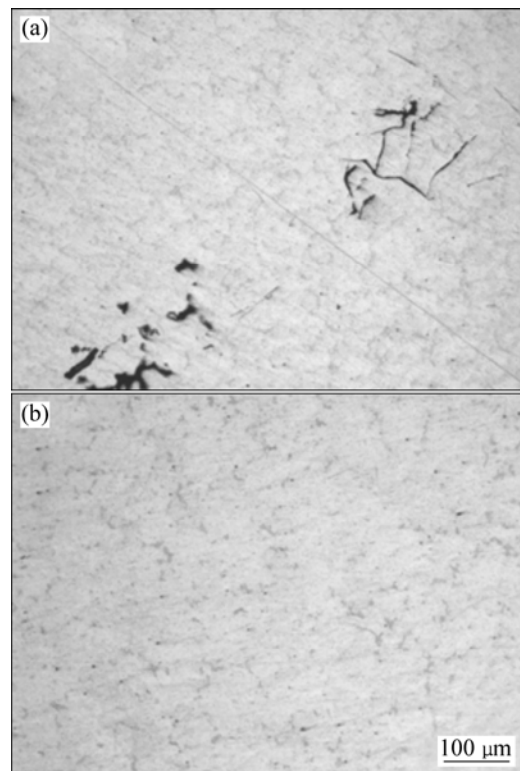


Fig.1 Morphologies of inclusions in Mg-Gd-Y-Zr alloy: (a) Without filtration; (b) With filtration (filter pore size of 150 μm)

The average size and volume fraction of inclusions in the alloy by different purification treatments are shown in Fig.2. It reveals that the average size and volume fraction decrease with the decrease of filter pore size. The average size decreases from 12.7 μm to 4.3 μm and the volume fraction from 0.26% to 0.06%, when the

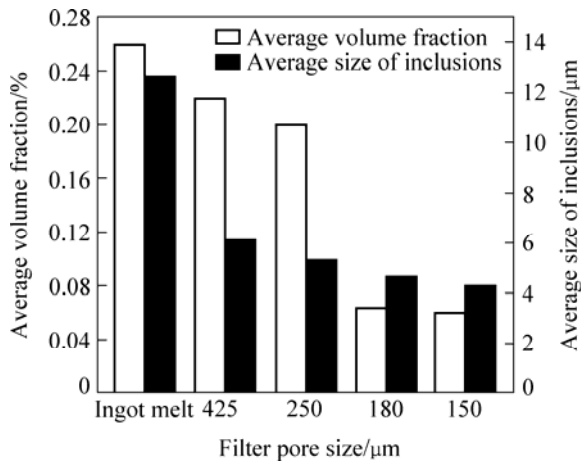


Fig.2 Effect of different filtering purification treatments on inclusion size and volume fraction

filter pore size reduces from 425 μm to 150 μm. The statistical results are consistent with the metallography results of the alloy, which indicates that the alloy is purified effectively by filtering.

3.2 Mechanical properties

Fig.3 shows the effect of purification treatment on mechanical properties of the alloy. Compared with the unpurified specimens, the ultimate tensile strength (σ_b), yield strength ($\sigma_{0.2}$) and elongation (δ) of the alloy with purification treatments in as-cast state are improved with the decrease of the average size and volume fraction of inclusions in the alloy. When the average size and volume fraction of inclusions decrease from 12.7 μm and 0.26% to 4.3 μm and 0.06%, the σ_b , $\sigma_{0.2}$ and δ of the alloy are enhanced from 200 MPa, 156 MPa and 3.4% to 232 MPa, 167 MPa and 7.0% by 16.5%, 6.7% and 105.9%, respectively. With the decrease of the average size and volume fraction of inclusions, σ_b and δ are increased gradually, but after increasing to 167 MPa, $\sigma_{0.2}$ is not influenced by the average size and volume fraction of inclusions effectively.

The fracture surfaces of the specimens in as-cast condition after tensile tests are shown in Fig.4. It can be seen that the fracture pattern has not been changed by filtering process. The fracture is still cleavage crack. It is found that there is an inclusion of about 20 μm entrapped in a pore on the fracture surface of the unpurified specimen (Fig.4(a)). The EDS analysis for the inclusion is given in Fig.5, which shows the inclusion is a typical flux inclusion, because the compositions include a lot of Cl, K and Ca. The inclusions entrapped in the matrix provide a notch effect during the tensile test, so they become fracture origin, which is the crucial factor affecting the fracture behavior[5, 14]. The size and distribution of the inclusions affect the tensile properties

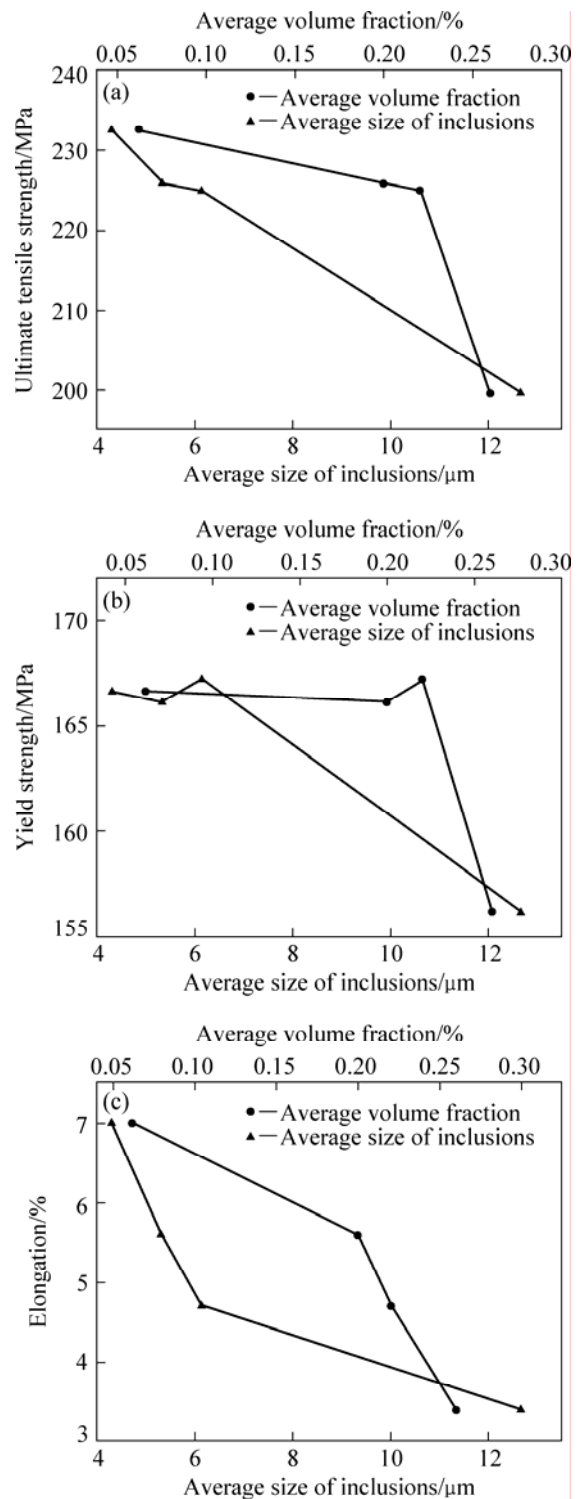


Fig.3 Effect of average size and volume fraction of inclusions on mechanical properties of alloy: (a) Ultimate tensile strength; (b) Yield strength; (c) Elongation

of the alloy[15]. The difference is that more inclusions exist in small and deep pores for specimens before purification than those for specimens after purification.

3.3 Corrosion resistance

Fig.6 shows the morphological characteristics of the

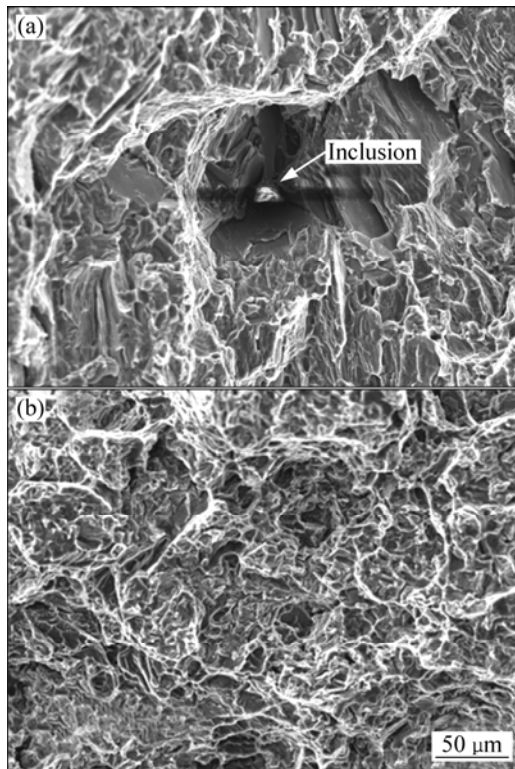


Fig.4 Fractographs of tensile samples of Mg-Gd-Y-Zr alloy in as-cast states: (a) Without filtration; (b) With filtration (filter pore size of 150 μm)

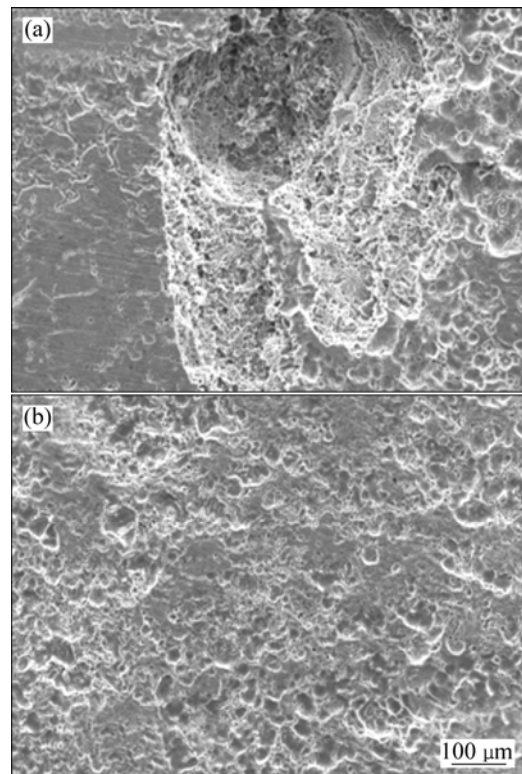


Fig.6 Surface morphologies of magnesium alloys after salt spray test: (a) Without filtration; (b) With filtration (filter pore size of 150 μm)

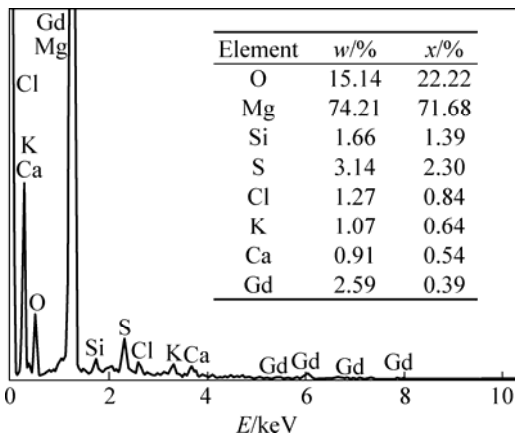


Fig.5 EDS analysis result of inclusion

corroded specimens after the salt spray test for 6 d. Deep corrosion pits are distributed on the surface of specimens, except for the ones purified with filtering. The corrosion rates of the alloy treated with different purification processes are shown in Fig.7. After the purification process with filter pore size of 450 μm , the average size and volume fraction of inclusions in the alloy decrease from 12.7 μm and 0.26% to 6.1 μm and 0.22%, and the corrosion rate decreases dramatically from 38.8 $\text{g}/(\text{m}^2\cdot\text{d})$ to 4.5 $\text{g}/(\text{m}^2\cdot\text{d})$. The corrosion property of the alloy is improved effectively by the purification. When the average size and volume fraction of inclusions continue

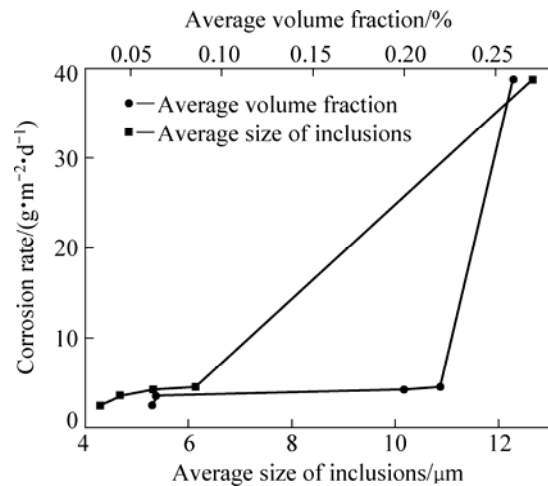


Fig.7 Effect of different purification treatments on corrosion rates of Mg-Gd-Y-Zr alloy

to decrease to 4.3 μm and 0.06%, the corrosion rate of the alloy decreases to 2.5 $\text{g}/(\text{m}^2\cdot\text{d})$ gradually. The deleterious effects of inclusions on corrosion resistance of magnesium alloys can be attributed to the formation of galvanic coupling between the inclusions and magnesium matrix[16], which accelerates the corrosion rate. The specimens purified by filtering exhibit excellent corrosion resistance, because the decrease of inclusion amounts in the alloy reduces the cathode areas and improves the corrosion resistance of the alloy.

4 Conclusions

1) The filtering method is an effective method to purify the Mg-Gd-Y-Zr alloy. By this method, not only the inclusions are removed but also the distribution of the left finer inclusions is improved in the alloy.

2) The mechanical properties of the Mg-Gd-Y-Zr alloy are greatly improved by the purification treatment. The ultimate tensile strength, yield strength and elongation of the cast Mg-Gd-Y-Zr alloy reach 232 MPa, 167 MPa, and 7.0%, respectively.

3) The corrosion rate of the purified cast Mg-Gd-Y-Zr alloy decreases from 38.8 g/(m²·d) to 2.5 g/(m²·d).

References

- [1] HE S M, ZENG X Q, PENG L M, GAO X, NIE J F, DING W J. Microstructure and strengthening mechanism of high strength Mg-10Gd-2Y-0.5Zr alloy [J]. *Journal of Alloys and Compounds*, 2007, 427(1/2): 316–323.
- [2] STUMPHY B, MUDRYK Y, RUSSELL A, HERMAN D, GSCHNEIDNER K Jr. Oxidation resistance of B2 rare earth-magnesium intermetallic compounds[J]. *Journal of Alloys and Compounds*, 2008, 460(1/2): 363–367.
- [3] HU H, LUO A. Inclusions in molten magnesium and potential assessment techniques [J]. *JOM*, 1996, 48(10): 47–51.
- [4] JUNG H C, LEE Y C, SHIN K S. Fluxless recycling of die-cast AZ91 magnesium alloy scrap [J]. *Materials Science Forum*, 2005, 475/479: 541–544.
- [5] KITAHARA Y, SHIMAZAKI H, YABU T, NOGUCHI H, SAKAMOTO M, UENO H. Influence of inclusions on fatigue characteristics of non-combustible Mg alloy [J]. *Materials Science Forum*, 2005, 482: 359–362.
- [6] ZHANG L F, DUPONT T. State of the art in the refining and recycling of magnesium [J]. *Materials Science Forum*, 2007, 546/549: 25–36.
- [7] GAO Hong-tao, WU Guo-hua, DING Wen-jiang, ZHU Yan-ping. Purifying effect of new flux on magnesium alloy [J]. *Trans Nonferrous Met Soc China*, 2004, 14(3): 530–536.
- [8] BAKKE P, ENGH T A, BATHEN E, ØYMO D, NORDMARK A. Magnesium filtration with ceramic foam filters and subsequent quantitative microscopy of the filters [J]. *Materials and Manufacturing Process*, 1994, 9(1): 111–138.
- [9] HILLIS J E. Magnesium recycling: Flux versus flux-free processes principles, advantages and disadvantages [C]//Proceeding of The 64th Annual World Magnesium Conference. British Columbia, Canada, 2007: 55–66.
- [10] WU G H, SEUNG H K, BONG S Y, CHANG D Y. Effects of non-flux purification on the microstructure and mechanical properties of AZ31+xCa Mg alloy [J]. *Materials Science Forum*, 2007, 546/549: 217–220.
- [11] WANG Wei, HUANG Yu-guang, WU Guo-hua, WANG Qu-dong, SUN Ming, DING Wen-jiang. Influence of flux containing YCl₃ additions on purifying effectiveness and properties of Mg-10Gd-3Y-0.5Zr alloy [J]. *Journal of Alloys and Compounds*, 2009, 480(2): 386–391.
- [12] WANG Wei, WU Guo-hua, WANG Qu-dong, HUANG Yu-guang, DING Wen-jiang. Gd contents, mechanical and corrosion properties of Mg-10Gd-3Y-0.5Zr alloy purified by fluxes containing GdCl₃ additions[J]. *Materials Science and Engineering A*, 2009, 507(1/2): 207–214.
- [13] ASTM B117. Standard Test Method of Salt Spray Testing [S]. Philadelphia, PA: ASTM, 1990: 20–26.
- [14] HORSTEMEYER M F, YANG N, GALL K, MCDOWELL D L, FAN J, GULLETT P M. High cycle fatigue of a die cast AZ91E-T4 magnesium alloy [J]. *Acta Materialia*, 2004, 52(5): 1327–1336.
- [15] SHIH T S, LIU W S, CHEN Y J. Fatigue of as-extruded AZ61A magnesium alloy [J]. *Materials Science and Engineering A*, 2002, 325(1/2): 152–162.
- [16] GAO Hong-tao, WU Guo-hua, DING Wen-jiang, LIU Liu-fa, ZENG Xiao-qin, ZHU Yan-ping. Study on Fe reduction in AZ91 melt by B₂O₃ [J]. *Materials Science and Engineering A*, 2004, 368(1/2): 311–317.

(Edited by YANG Bing)